Journal of Advanced Research 62 (2024) 187–198

Contents lists available at ScienceDirect

Journal of Advanced Research

journal homepage: www.elsevier.com/locate/jare

Original Article

Calcium influx: An essential process by which α-Synuclein regulates morphology of erythrocytes

Ying Yang [a,b,1], Min Shi [c,1], Xiaodan Liu [b,1], Qiaoyun Zhu [d], Zhi Xu [a], Genliang Liu [e,f], Tao Feng [e,f,*], Tessandra Stewart [c,*], Jing Zhang [a,g,*]

[a] Department of Pathology, Zhejiang University First Affiliated Hospital and School of Medicine, Hangzhou, Zhejiang 310002, China
[b] Department of Pathology, School of Basic Medical Sciences, Peking University Third Hospital, Peking University Health Science Center, Beijing 100191, China
[c] Department of Laboratory Medicine and Pathology, University of Washington School of Medicine, Seattle, WA 98104, USA
[d] Central Laboratory, Zhejiang University First Affiliated Hospital and School of Medicine, Hangzhou, Zhejiang 310002, China
[e] Center for Movement Disorders, Department of Neurology, Beijing Tiantan Hospital, Capital Medical University, Beijing 100070, China
[f] China National Clinical Research Center for Neurological Diseases, Beijing 100070, China
[g] National Human Brain Bank for Health and Disease, Zhejiang University, Zhejiang, Hangzhou, China

HIGHLIGHTS

- Morphological abnormalities of RBCs were observed in PD patients.
- Increased aggregated α-syn in RBC membrane were observed in PD patients.
- A decreased proportion of normal RBCs and increased aggregated α-syn in RBC membrane were also observed in PD model mice.
- Treating RBCs derived from SNCA knockout mice with aggregated α-syn resulted in a higher percentage of acanthocytes.
- Applying aggregated α-syn to RBC membrane directly induced extracellular calcium influx along with morphological changes.

GRAPHICAL ABSTRACT

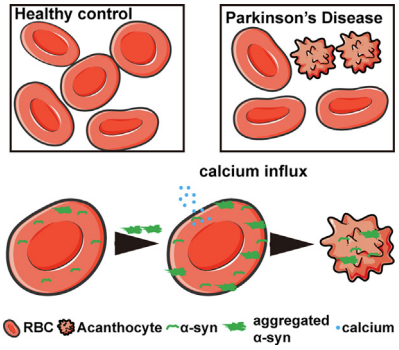

ARTICLE INFO

Article history:
Received 18 July 2022
Revised 6 September 2023
Accepted 11 September 2023
Available online 13 September 2023

Keywords:
Red blood cells
α-synuclein
Parkinson's disease
Calcium influx

ABSTRACT

Introduction: Morphological abnormalities of erythrocytes/red blood cells (RBCs), e.g., increased acanthocytes, in Parkinson's disease (PD) have been reported previously, although the underlying mechanisms remain to be characterized. In this study, the potential roles of α-synuclein (α-syn), a protein critically involved in PD and highly abundant in RBCs, were studied in PD patients as well as in a PD mouse model.
Methods: Transgenic [PAC-Tg ($SNCA^{A53T}$), A53T] mice overexpressing A53T mutant α-syn and SNCA knockout mice were employed to characterize the effect of α-syn on RBC morphology. In addition to A53T and *SNCA* knockout mice, the morphology of RBCs of PD patients was also examined using scanning electron microscopy. The potential roles of α-syn were further investigated in cultured RBCs and mice.
Results: Morphological abnormalities of RBCs and increased accumulation of aggregated α-syn on the RBC membrane were observed in PD patients. A similar phenomenon was also observed in A53T mice. Furthermore, while mice lacking α-syn expression showed a lower proportion of acanthocytes, treating RBCs derived from *SNCA* knockout mice with aggregated α-syn resulted in a higher percentage of

* Corresponding authors at: Zhejiang University First Affiliated Hospital and School of Medicine, China (J. Zhang). University of Washington School of Medicine, USA (T. Stewart). Beijing Tiantan Hospital, Capital Medical University China (T. Feng).
E-mail addresses: happyft@sina.com (T. Feng), stewarth@uw.edu (T. Stewart), jzhang1989@zju.edu.cn (J. Zhang).
[1] These authors contributed equally to this work.

https://doi.org/10.1016/j.jare.2023.09.009

acanthocytes. In a follow-up proteomic investigation, several major classes of proteins were identified as α-syn-associated proteins on the RBC membrane, seven of which were calcium-binding proteins. Applying aggregated α-syn to the RBC membrane directly induced extracellular calcium influx along with morphological changes; both observations were adequately reversed by blocking calcium influx.
Conclusions: This study demonstrated that α-syn plays a critical role in PD-associated morphological abnormalities of RBCs, at least partially via a process mediated by extracellular calcium influx.

Introduction

Parkinson's disease (PD), a chronic and age-related slowly progressive neurodegenerative disorder, is characterized by a variable combination of motor and non-motor symptoms [1–3]. α-Synuclein (α-syn), a major component of Lewy bodies, is a key protein critically involved in the pathogenesis of PD [4,5]. In addition to central nervous system (CNS), α-syn is also expressed in other parts of the body, especially in the blood. Red blood cells (RBCs) or erythrocytes contain over 99% of blood's α-syn, reaching a concentration much higher than that observed in the cerebrospinal fluid (CSF) [6–8]. Oligomeric α-syn, the toxic form of α-syn [9–11], is reported to be higher in RBCs of PD patients compared to controls [12,13]. Furthermore, the levels of total and aggregated α-syn are significantly higher in the RBC membrane fractions of PD patients compared to those of healthy controls [8]. Previously, α-syn is reported to be associated with heightened oxidative stress, disrupted axonal transport, dysfunction in the ubiquitin-proteasome system, impaired mitochondrial function, and synaptic issues [14,15]. However, until recent years, α-syn still lacks a definitively recognized function. Despite its remarkable conservation throughout vertebrate evolution, it does not exhibit substantial similarity to any protein with an established function. Consequently, the role of both monomeric and aggregated forms of α-syn found within RBCs remains entirely unknown.

Previously, a study reported that the RBCs of PD patients often exhibit abnormalities, characterized by an increased presence of acanthocytes, which are cells displaying surface membrane protrusions [16]. Furthermore, PD is frequently associated with anemia [17–19], and recent research in a population-based cohort has shown that newly diagnosed anemic patients face a higher risk of developing PD compared to non-anemic individuals [17]. Given the substantial presence of α-syn in RBCs and its central role in PD, it becomes imperative to probe into the potential involvement of α-syn in the PD-related morphological alterations of RBCs and anemia. It has been suggested that α-syn is able to interact with lipid membranes, and increasing evidence has demonstrated that: 1) lipid membranes have the capacity to foster α-syn aggregation; and 2) the aggregation of α-syn on the membrane can swiftly disturb membrane integrity [20–22]. Structural analysis of α-syn oligomers has revealed that these species harbor a highly lipophilic element involved in interactions with the membrane and perturb membrane integrity through insertion of a structured region into the lipid bilayers [23].

To investigate the potential role of α-syn in RBC, we analyzed the morphology of RBCs from individuals with PD and other neurodegenerative diseases, discovering RBC morphological abnormalities only in PD patients. A similar phenomenon was also observed in PD model mice overexpressing the A53T mutant α-syn. To test the hypothesis that aggregated α-syn on the RBC membrane may impact RBC morphology in PD and investigate the mechanisms underlying this pathogenic phenomenon, we utilized *SNCA* (the gene encoding α-syn) knockout mice (SNCA-KO) to demonstrate that the RBC morphological abnormalities were clearly associated with aggregated α-syn. Further investigation has revealed that an elevated presence of aggregated α-syn on the RBC membrane might trigger an influx of extracellular calcium, subsequently leading to alterations in RBC morphology within PD. These findings suggest that α-syn plays a critical role in PD-associated morphological abnormalities of RBCs through a process likely mediated by extracellular calcium influx.

Methods

Human subjects and sample collection

The study was approved by the Clinical Research Ethics Committee of the First Affiliated Hospital, Zhejiang University School of Medicine (No. IIT20200473A). Blood samples from a total of 72 subjects, including 26 patients with PD, 13 patients with Alzheimer's disease (AD), 5 patients with mild cognitive impairment (MCI), 2 patients with essential tremor (ET), and 26 healthy controls whose ages and sexes were matched with those of PD patients, were derived from Beijing Tiantan Hospital and the First Affiliated Hospital, Zhejiang University School of Medicine, for RBC morphology assessments in this study. The contributing hospitals obtained ethics approval before study enrollment, and all participants provided written informed consent for blood sampling as well as permission to use their clinical information for research purposes. The data of demographics and clinical information of the participants is shown in Supplementary Table 1.

Animals and antibodies

All experiments involving mice were approved by the Animal Care and Use Committee of the animal facility at Zhejiang University School of Medicine (20221077). The mice used in this study, including *SNCA* knockout mice (SNCA-KO mice, B6;129X1-Snca^{tm1Rosl} /J, strain number: 003692), and PD model mice (A53T mice, dbl-PAC-Tg(SNCA^{A53T}); SNCA $^{-/-}$, strain number: 010799), were purchased from the Jackson Laboratory, while wild-type mice (WT mice, C57BL/6J) were obtained from Hangzhou Ziyuan Biotechnology LTD. Both SNCA-KO mice and PD model mice lack endogenous α-syn expression, whereas the PD model mice expressed the human α-syn with the A53T mutation peripherally. The mice were raised in a specific pathogen-free standard environment under a 12-hour light–dark cycle, with free access to food and water. Blood was collected after anesthesia and stored in syringes primed with 15% EDTA, which was then rapidly fixed in glutaraldehyde for morphological studies, or centrifuged at 1000 *g* for 15 min for further analysis.

The following antibodies were used for western blot (WB), immunofluorescence (IF), and immunoprecipitation (IP): Rabbit monoclonal [EPR20535] to Alpha-synuclein (ab212184, Abcam) for WB; rabbit monoclonal [MJFR1] to Alpha-synuclein (ab209420, Abcam) for IP; rabbit monoclonal conformation-specific [MJFR-14-6-4-2] to aggregated α-synuclein (ab209538, Abcam) for WB; mouse polyclonal against glyceraldehyde-3-phosphate dehydrogenase (GAPDH, HC301, TRANS) for WB; mouse

monoclonal (JC159) against glycophorin A (CD235a, MA5-12484, Invitrogen) for WB; rabbit monoclonal [EP1845Y] to Sodium Potassium ATPase (ab76020, Abcam) for IF. Alexa Fluor 555, 488, or 633 conjugated secondary antibodies, and horseradish peroxidase (HRP)-conjugated secondary antibodies used in IF and WB, were purchased from Thermo Fisher Scientific.

Scanning electron microscopy (SEM)

Human/mouse blood samples and mouse RBCs treated with monomeric α-syn, aggregated α-syn, or vehicle (PBS) for 48 h were collected by centrifuging at 1000 *g* for 5 min and immediately fixed with 2.5% glutaraldehyde. The RBC samples were dehydrated using an acetone gradient ranging from 30% to 100%, followed by 50%, 67%, and 75% araldite in acetone, then mounted onto aluminum stubs using conductive carbon tape, and coated with platinum in a JEOL JEC-3000FC auto fine coater. Photomicrographs were captured using an FE-SEM JEOL JSM-7900F. Fifteen to twenty SEM images were acquired for each RBC sample. Biconcave disc-shaped RBCs were categorized as normal RBCs, RBCs with prominent thorn-like surface protrusions were classified as acanthocytes, and biconcave RBCs without disc-shape and surface protrusions were identified as abnormal RBCs. A total of 1000 RBCs from 10 blinded SEM images were counted for each individual.

RBC collection and separation

Human or mouse blood was collected in EDTA-coated anticoagulant tubes and then centrifuged at 1000 *g* for 10 min. The plasma and leukocyte layers were removed, and the RBCs were pelleted. Subsequently, the RBCs were washed 3 times with PBS and immediately processed for membrane and cytosol separation. For the separation of RBC fractions, the RBCs underwent five sequential freeze (−80 °C) and thaw (25 °C) cycles. Following this, the samples were centrifuged at 16,000 *g* for 15 min. The supernatant was collected as the cytosolic fraction, while the pellet was further washed 3 times with PBS, incubated with STET lysis buffer (R20994, Shanghai Yuanye Bio-Technology Co., Ltd), and collected as the membrane fraction. The efficiency of the RBCs separation was verified through WB with membrane (CD235a) and cytoplasmic (GAPDH) proteins.

Meso scale discovery immunoassays

The levels of α-syn on the RBC membrane and cytosolic fractions were assessed using a well-established method, following previously described protocols [8,24]. Firstly, the capturing antibodies (anti-α-syn antibody MJFR1(ab138591, Abcam) for total α-syn or anti-α-syn filaments MJFR-14 (ab209538, Abcam) for aggregated α-syn) were biotinylated, linker-conjugated, and coated onto standard 96-well U-Plex plates (Meso scale discovery). Then, the RBC membrane samples, cytosolic samples, and calibrator (recombinant α-syn, Sino biological, and aggregated α-syn, Proteose) were diluted by Diluent 35 and added into the plate (total 5 μg protein,100 μl/well). After incubation overnight, the plate was washed 3 times using washing buffer. The sulfo-TAG-labeled anti-α-syn antibody (BD42) was used as the detecting antibody (1 ng/ml) and prepared in dilution buffer (0.1% bovine serum albumin (BSA) in PBS). After incubation with detecting antibody and reading buffer T sequentially, the plate was read and analyzed using a Quickplex SQ 120 (Meso scale discovery, USA).

Western blot (WB)

Proteins were extracted using RIPA cell lysis buffer (APPLYGEN, C1053) and quantified using the BCA Protein Assay Kit (APPLYGEN, P1511) following the manufacturer's instruction. RBC lysates (∼40 μg of total protein) or α-syn samples (∼10 ng) were loaded onto a 4–12% Criterion™ TGX Stain-Free™ Protein Gel (Bio-Rad Laboratories) before being transferred to a PVDF membrane (Merck Millipore, 4515). The membranes were blocked with 5% skim milk and then probed with corresponding primary antibodies. After washing, the membranes were incubated with appropriate horseradish peroxidase (HRP)-conjugated secondary antibodies and visualized using Immobilon Western Chemiluminescent HRP Substrate (WBKLS0500, Merck Millipore) via the ChemiDoc XRS$^+$ System (Bio-Rad). The quantification of bands was performed using Image J.

In vitro aggregation assays

The *in vitro* aggregation experiments were conducted following a previously described protocol [25]. Briefly, 1 μg/μl full-length monomeric α-syn (12093-HNAE, Sino Biological) was incubated at 37 °C with shaking using Multiscan GO (Thermo Fisher) for 120 h.

In vitro RBC cultures

RBCs from SNCA-KO mice, A53T mice, or age-matched WT mice were cultured in RPMI-1640 medium. RBCs were treated with 0.15–4.5 μg/ml monomeric or aggregated α-syn or PBS (vehicle control) and cultured at 37 °C in an incubator for 48 h. After incubation, RBCs were collected by centrifuging at 1500 *g* for 10 min.

Immunofluorescence (IF) staining

RBCs treated with monomeric or aggregated α-syn were fixed in 4% paraformaldehyde solution for 15 min, washed with PBS buffer, and incubated with blocking solution (1% BSA, 4% goat serum, and 0.3% Triton X-100 in PBS) for 1 h. Next, RBCs were incubated with appropriate primary antibodies overnight at 4 °C, then washed with washing buffer (0.1% Triton X-100 in PBS, PBST), and incubated with corresponding secondary antibodies diluted in PBST for 3 h. Then, the RBCs were embedded in Vectashield medium. IF images were captured with a Zeiss instrument under 20× or 40× magnification.

Real-time quaking-induced conversion (RT-QuIC)

The RT-QuIC assay was carried out as in previous studies [26–28]. Firstly, 100 mmol/L phosphate buffer (pH 8.2), 10 μM Thioflavin T (ThT), 200 μg/ml full length monomeric WT α-syn (RPB222Mu02, Cloud-clone), and 100 μg total protein from RBC lysates were added to a microplate as the RT-QuIC assay mixture. Each sample was run in duplicate. Two negative controls (reactions without adding RBC lysates) and two empty controls were included. The plate was incubated in a CLARIOstar high-performance microplate reader (BMG LABTECH, Germany) at 30 °C for 120 h with intermittent shaking cycles: 1-min shake (200 rpm),14-min rest, and ThT fluorescence measurement once (445 nm excitation and 485 nm emission). A positive response was defined as a relative fluorescence (RFU) above the mean of the negative controls in 120 h.

Phenylhydrazine (PHZ) treatment

12-month-old WT mice received a solitary intraperitoneal injection of 30 mg/kg PHZ, with the control group receiving an injection of normal saline. Automated hematology analyzers were employed to assess the RBC count and mean corpuscular hemoglobin concentration (MCHC).

Analysis of α-syn-associated proteins by liquid Chromatography-Mass spectrometry (LC-MS/MS)

RBC ghost preparation: 200 μl aliquots of the RBC pellet from 3 healthy individuals were pooled. RBC ghosts were prepared by adding 9 ml of 10 mM phosphate buffer, pH 7.4, with 1 mM phenyl methyl sulfonyl fluoride (PMSF), and then centrifuged at 39,000 *g* for 30 min. Immunoprecipitation of α-syn-associated proteins: The anti-α-syn antibody (MJFR1, ab209420, Abcam) was coupled with Dynabeads (Invitrogen™, 14311D) following the manufacturer's instruction. 1000 μg RBC membrane protein was added to 100 μl α-syn antibody-coupled beads and incubated overnight. After incubation, the beads were washed with lysis buffer three times and then washed with washing buffer (50 mM TEAB, 50 mM Tris pH 8.5, 1 mM EGTA, and 75 mM KCl). After the supernatant was removed, the α-syn-associated proteins were eluted with urea elution buffer (50 mM TEAB with 8 M urea). LC-MS/MS: The α-syn-associated proteins were digested overnight with trypsin solution (25 μg/ml). 0.8 mg TMT in 41 μl acetonitrile was added to 100 μl of digested peptides for 1 h at room temperature. The reaction was stopped by 8 μl 5% hydroxylamine for 15 min. The peptides were then applied to Pierce™ Peptide Desalting Spin Columns (Thermo Scientific, 89852) and dried using a centrifugal vacuum. LC-MS/MS analysis was performed using an UltiMate 3000 nanoLC (Thermo Scientific) coupled with an Orbitrap Exploris 480 mass spectrometer (Thermo Scientific). LC-MS/MS data were processed using Proteome Discoverer software suite v.2.5. Database search was conducted using the Sequest search engine. Spectra were searched against a SwissProt Homo sapiens database concatenated with a reverse decoy database. Trypsin/P was specified as the cleavage enzyme, allowing up to 2 missing cleavages. The false discovery rate (FDR) was set to 1% on PSM and peptide levels. TMT-10plex quantification was performed. The gene ontology (GO) and functional categorization of the α-syn-associated proteins detected by MS were performed using PANTHER classification system (http://pantherdb.org/). The list of the original α-syn-associated proteins identified by LC-MS is presented in Supplementary Table 2.

Measurement of intracellular Ca^{2+}

RBCs were seeded at a density of 6×10^5 cells/cm^2 on 20 mm confocal petri dishes (430165, Corning) precoated with poly-D-lysin/laminin and cultured with RPMI-1640 medium. One day later, RBCs were proceeded for Ca^{2+} measurements. The RBCs were washed with Ringer buffer and then incubated with 2 μM of the cell-permeable Fluo-4 AM dye (HY-101896, MCE) in Ringer buffer at 37 °C for 1 h. Subsequently, RBCs were treated with 0.15 μg/ml, 0.75 μg/ml, and 4.5 μg/ml of monomeric α-syn, aggregated α-syn, or PBS. The measurements were conducted using a confocal microscope (TCS-SP8, Leica). Time-lapse pictures were captured every 5 s. Signals were expressed in RFUs. The recording duration was 300 s. Before Ca^{2+} measurements, 10 μM Amlodipine (HY-B0317, MCE), 50 nM ω-Conotoxin GVIA TFA (HY-P0189A, MCE), or 1 μM Fendiline hydrochloride (HY-B0984, MCE) were added.

Statistical analyses

Statistical analyses were conducted with GraphPad Prism 9. All results were presented as mean ± standard error of the mean (SEM). The unpaired two-tailed Student's *t*-test was used for two group comparisons, and the one-way ANOVA was used for multiple comparisons.

Data sharing

The data that supports the findings of this study are available in the supplementary material of this article.

Results

Altered morphology of RBCs in PD patients accompanied by increased membrane-bound aggregated α-syn

To systematically assess morphological alterations in the RBCs of PD patients, fresh RBC samples were obtained from patients with PD (n = 26), age- and gender-matched healthy control (n = 26), and neurological disease controls, including patients with essential tremor (ET, n = 2), or patients with cognitive impairments such as Alzheimer's disease (AD, n = 13) and mild cognitive impairment (MCI, n = 5) (Supplementary Table 1). The samples were analyzed using scanning electron microscopy (SEM), revealing that the RBCs of healthy controls were generally biconcave disc-shaped (Fig. 1**A**), while a significant portion of the RBCs of PD patients were deformed, featuring protrusions on the surface (Fig. 1**B**), i.e., the formation of acanthocytes. The percentage of normally shaped RBCs was significantly lower in PD patients compared to healthy controls ($P < 0.001$), while those from patients with ET, AD, or MCI were not significantly different from healthy controls (Fig. 1**C–F**). These results suggest that the morphology of RBCs might be altered specifically in PD patients, rather than as a general consequence of neurodegeneration.

Given the high level of α-syn in RBCs, as well as the role of α-syn in PD, we next sought to investigate whether α-syn participates in the mechanisms underlying PD-related morphological alterations of RBCs. The levels of total and aggregated α-syn in RBCs from PD patients and healthy controls were measured using a well-established Meso Scale Discovery immunoassay [8,24]. The level of total α-syn associated with the RBC membrane of PD patients showed a trend towards being higher when compared to that in healthy controls, but this difference did not reach statistical significance ($P = 0.066$) (Fig. 1**G** and **Fig. S1**). In contrast, the level of membrane-bound aggregated α-syn from RBCs of PD patients was significantly higher than that in healthy controls ($P < 0.001$) (Fig. 1**H**). There were no significant differences observed in either the total or aggregated α-syn levels in the cytosol of RBCs when comparing PD patients with healthy controls (Fig. 1**G–H**).

Altered morphology of RBCs in A53T mice and SNCA-KO mice

To further explore the relationship between aggregated α-syn in RBCs and their morphology, we examined the accumulation of aggregated α-syn in RBCs obtained from a PD mouse model (A53T mice), as well as from a SNCA knockout mouse model (SNCA-KO mice). These A53T mice conventionally demonstrate α-syn accumulation in the colon, along with early gastrointestinal dysfunction, before developing motor abnormalities between 6 and 12 months [29]. RBCs were collected from 1-, 3-, 6-, and 12-month-old WT and A53T mice. As shown in Fig. 2**A**, the RBCs of 1-month-old WT and A53T mice exhibited normal morphology. With increasing age, the number of normal shaped RBCs gradually decreased, and at each time point, the proportion of normal RBCs in A53T mice was significantly lower than that in WT mice (Fig. 2**B-C**). In line with the observations in human studies, the level of aggregated α-syn on the RBC membrane was significantly higher in A53T mice compared to WT mice (Fig. 2**D**). To further elucidate the impact of aggregated α-syn on RBC morphology, we examined the RBCs of SNCA-KO mice. WB results confirmed the absence of α-syn in RBCs of SNCA-KO mice (Fig. 2**E**). In contrast to A53T mice,

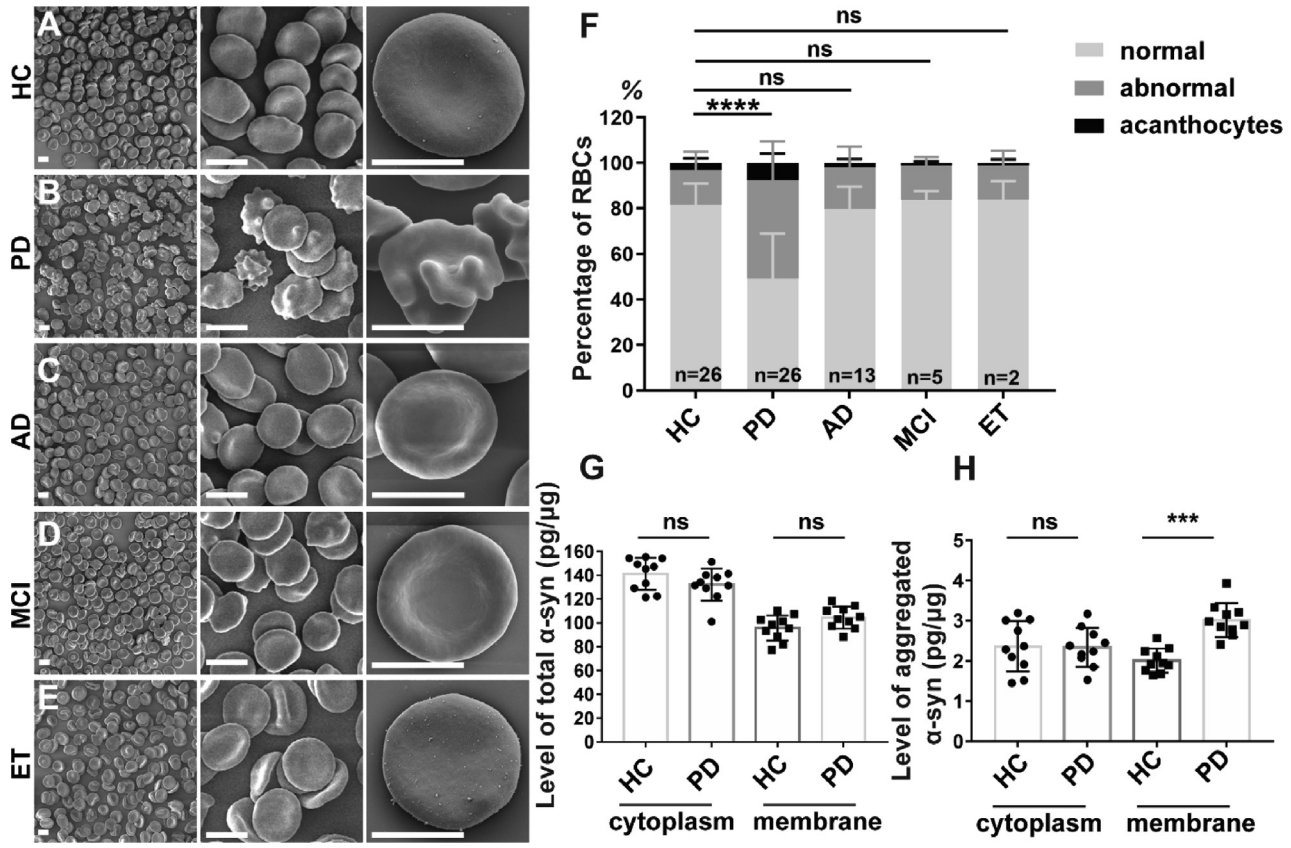

Fig. 1. Morphological abnormalities of RBCs in PD patients accompanied by increased membrane-bound aggregated α-syn. (**A**–**E**) Representative RBC images of healthy controls (HC) (**A**), patients with Parkinson's disease (PD) (**B**), patients with Alzheimer's disease (AD) (**C**), patients with mild cognitive impairment (MCI) (**D**), and patients with essential tremor patients (ET) (**E**). Scale bar: 3 μm. (**F**) The percentage of normally-shaped RBCs in the PD group was significantly different from that in the HC group. N = 1000 randomly selected RBCs counted from each individual. Statistical significance was calculated on the percentage of normal RBCs between patients and HC via one-way ANOVA followed by Tukey's post-hoc test. (**G**) The level of total α-syn in the cytosolic and membrane fractions of RBCs was examined in PD and HC. (**H**) The level of aggregated α-syn in the RBC cytosolic and membrane fractions was examined in PD and HC. Values are means ± S.E.M; ns, not significant; ***, $P < 0.001$; ****, $P < 0.0001$.

SEM findings showed that the proportion of RBCs with normal morphology in 6-month-old SNCA-KO mice was similar to that in WT mice (Fig. 2**F–G**), while the proportion of acanthocytes was significantly lower in SNCA-KO mice when compared to WT mice (Fig. 2**H**). Taken together, these results suggest a potential association between α-syn and altered RBC morphology, particularly the formation of acanthocytes, in PD.

Direct effect of α-syn on RBC morphology

To investigate whether α-syn could directly mediate morphological changes in RBCs, cultured RBCs from 3-month-old WT, SNCA-KO, and A53T mice were exposed to different concentrations of monomeric or aggregated α-syn *in vitro* (**Fig. S2**). IF analysis revealed the presence of monomeric or aggregated α-syn on the surface of RBCs (Fig. S3A). Notably, no significant difference in morphology was observed in RBCs from WT mice treated with monomeric α-syn when compared to those treated with PBS (Fig. 3**A, 3D, and** S3**B**). However, the morphology of the WT RBCs treated with aggregated α-syn exhibited a dose-dependent increase in the proportion of acanthocytes (Fig. 3**A, 3D, and** S3**B**).

The morphology of RBCs from SNCA-KO mice, when treated with α-syn, exhibited significant differences compared to WT RBCs, with two key observations: 1) the proportion of acanthocytes significantly increased even with monomeric α-syn treatment, and 2) this effect was even more pronounced with aggregated α-syn treatment, displaying a dose-dependent pattern, surpassing that of WT RBCs (Fig. 3**B and 3E**). Regarding the morphology of RBCs from A53T mice, the application of exogenous monomeric and aggregated α-syn had relatively modest exacerbating effects (Fig. 3**C and 3F**).

The potential impact of membrane-bound aggregated α-syn on RBC morphology

We postulated that the morphological alterations induced by aggregated α-syn in RBCs could be attributed to the continuous accumulation of α-syn aggregates on their membrane. To test this hypothesis, we employed phenyl hydrazine (PHZ), an oxidatively damaging hemolytic agent that causes acute RBC hemolysis in mice, triggering hematopoiesis to restore RBC levels [30]. We administered a single intraperitoneal injection of PHZ to 12-month-old WT mice. This intervention effectively restored RBCs to a relatively uniform early state, allowing us to monitor RBC morphology and the levels of α-syn aggregates over 120 days. Consistent with previous research [31], following the PHZ injection, the total RBC count in the mice gradually decreased, reaching its lowest level on the fifth day, concurrently with an increase in MCHC (**Fig. S4**). Subsequently, the total RBC count gradually rebounded and recovered to normal levels on the thirteenth day (Fig. S4A). Correspondingly, MCHC also returned to its baseline value by the thirteenth day (Fig. S4B).

To assess the relative level of aggregated α-syn in RBCs, we employed the real-time quaking-induced conversion (RT-QuIC) technique. This method can amplify proteins with self-aggregation properties, enabling us to compare the levels of

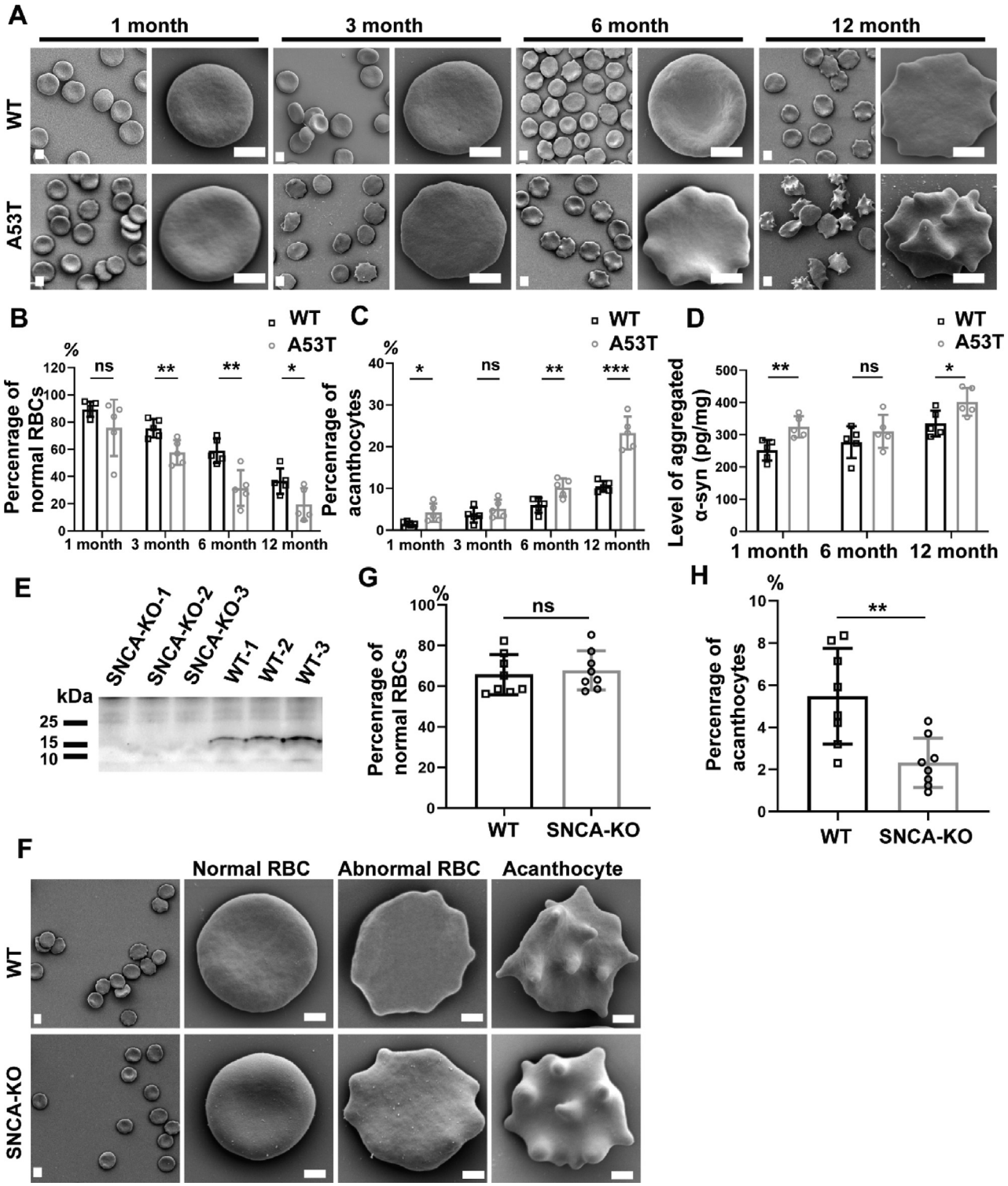

Fig. 2. Morphological abnormalities of RBCs and the expression of α-syn in A53T mice and SNCA-KO mice. (A) Scanning electron micrographs of RBCs of WT mice and A53T mice. Scale bar: 1 μm. **(B)** Proportion of normal RBCs in WT mice and A53T mice. **(C)** Proportion of acanthocytes in WT mice and A53T mice. N = 5 mice, 1000 randomly selected RBCs counted from each mouse. **(D)** The level of aggregated α-syn was examined in WT mice and A53T mice (N = 5). **(E)** Representative western blot images of α-syn in SNCA-KO mice. **(F)** Scanning electron micrograph showing the morphology of SNCA-KO RBCs. Scale bar: 500 nm. **(G)** No significant difference was observed in the proportion of RBCs with normal morphology in WT and SNCA-KO mice. **(H)** The proportion of acanthocytes in WT mice was significantly higher than in SNCA-KO mice. N = 8 mice, 1000 randomly selected RBCs counted for each mouse. Values are presented as means ± S.E.M; ns, not significant; *, $P < 0.05$; **, $P < 0.01$; ***, $P < 0.001$.

aggregation-promoting "seeds" in the original sample [26,27]. Using this technique, the RBC membrane sample collected on day 90 exhibited a faster positive response compared to the sample collected on day 30, indicating that the level of aggregated α-syn on the RBC membrane on day 90 was significantly higher than that on day 30 (Fig. 4**A**). From the perspective of RBC morphology, on day 30 after the PHZ injection, the proportion of RBCs with normal morphology was higher than that in the control group injected

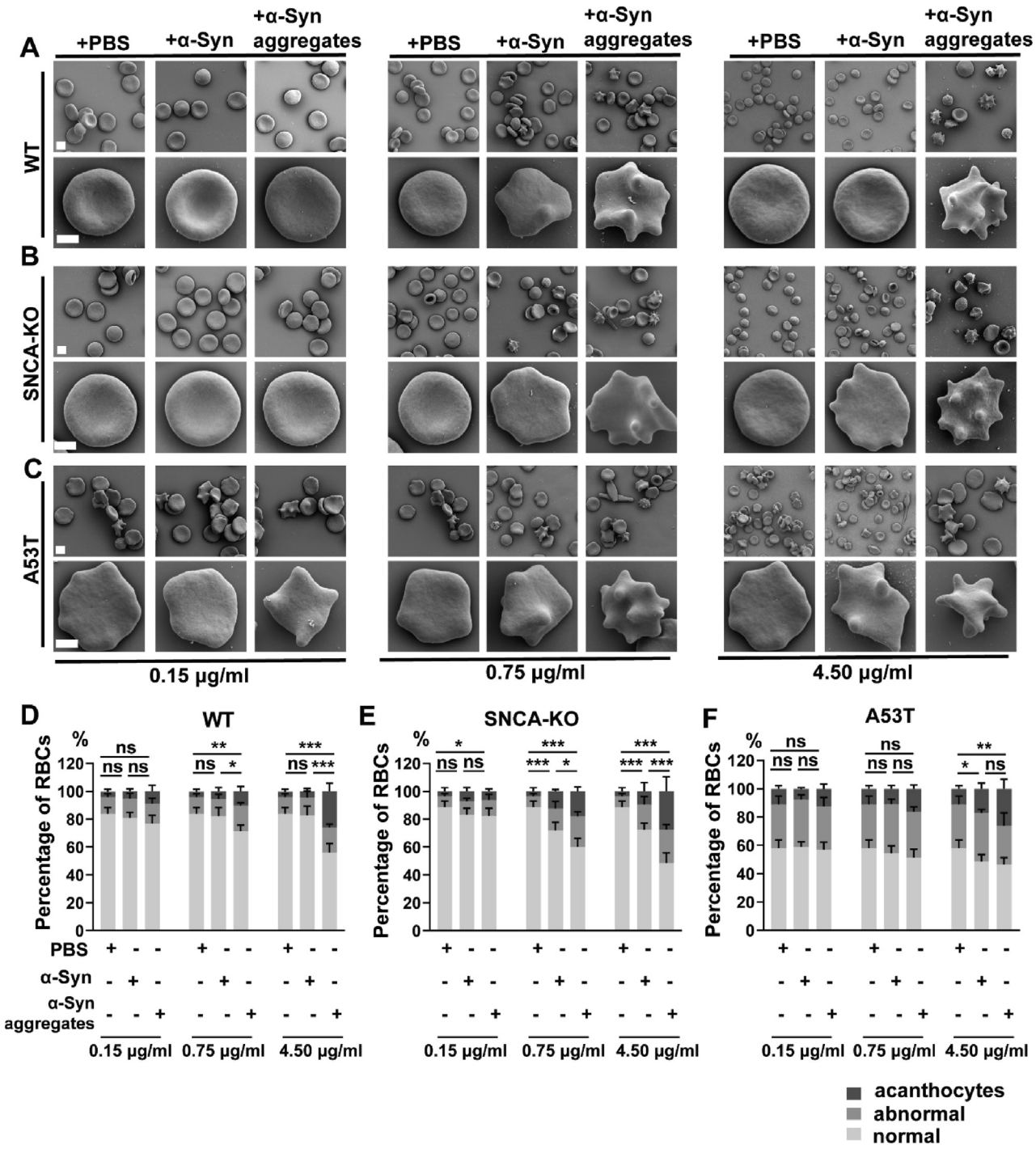

Fig. 3. The effect of α-syn on the morphology of RBCs. (A–C) Scanning electron micrographs show RBCs of WT mice (**A**), SNCA-KO mice (**B**), and A53T mice (**C**) treated with different concentrations of monomeric α-syn (α-syn) or aggregated α-syn (α-syn aggregates) for 48 h. Scale bar: 1 μm. **(D-F)** Comparison of the percentage of RBCs in WT mice (**D**), SNCA-KO mice (**E**), and A53T mice (**F**) treated with α-syn. N = 5 mice, 1000 randomly selected RBCs counted for each mouse. Statistical significance was calculated on the percentage of normal RBCs between certain groups via Student's *t*-test. Values are presented as means ± S.E.M; ns, not significant; *, $P < 0.05$; **, $P < 0.01$; ***, $P < 0.001$.

with normal saline (Fig. 4**B-C**). However, by day 90, the morphology of RBCs did not change significantly in the control group, while in the PHZ injection group, the proportion of RBCs with normal morphology decreased, and the proportion of acanthocytes increased (Fig. 4**D-E**). These findings lend support to the notion that the level of aggregated α-syn on RBCs can indeed influence RBC morphology.

Proteins associated with α-syn on the RBC membrane revealed by proteomic analysis

To further investigate the mechanism by which α-syn affects RBC morphology, RBC ghosts were prepared from fresh human RBCs, α-syn-interacting RBC membrane proteins were co-immunoprecipitated by α-syn antibody-coupled dynabeads, and

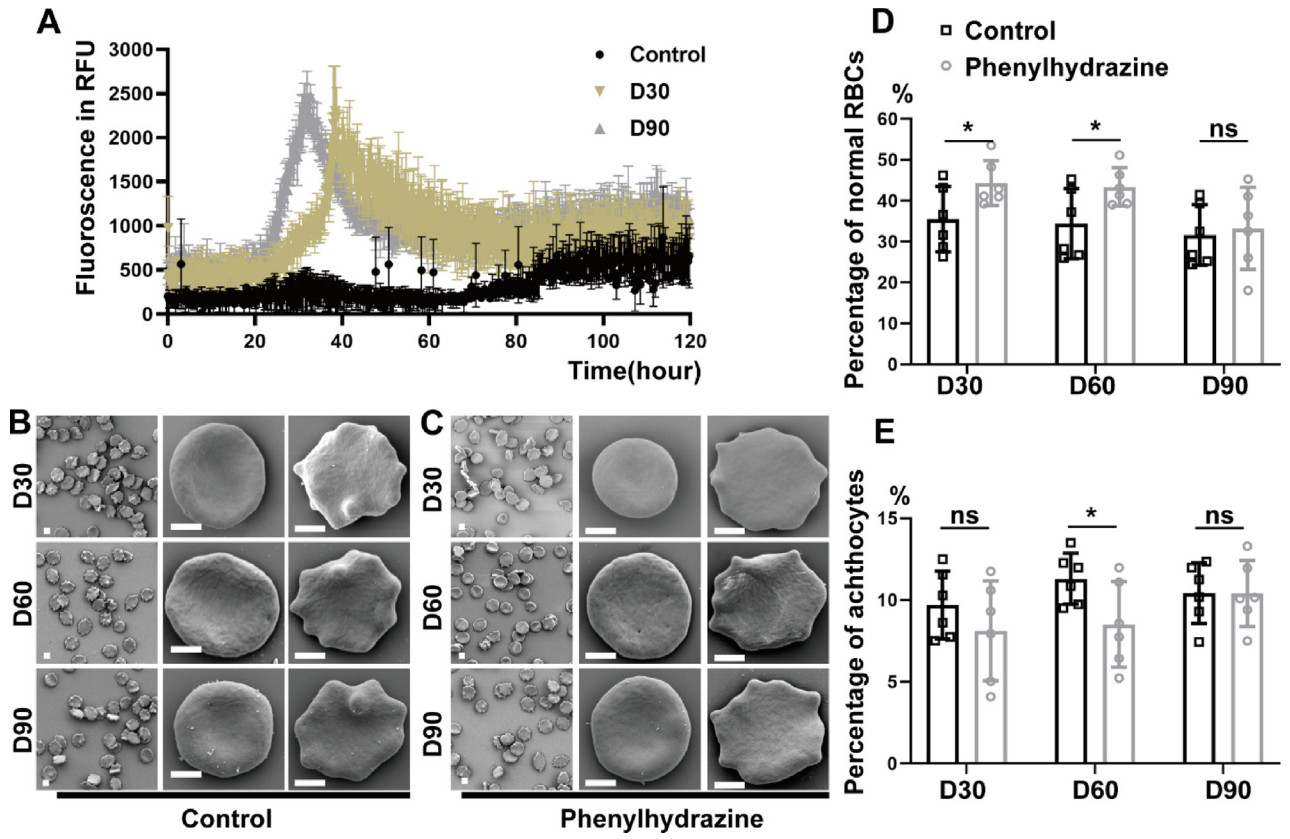

Fig. 4. The level of aggregated α-syn on the membrane of mouse RBCs might affect the RBC morphology. (A) RT-QuIC responses observed with reactions seeded with RBC samples of mice treated with PHZ. **(B)** The RBC morphology in blood samples of control group over time. Scale bar: 1 μm. (**C**) The RBC morphology in PHZ treatment group over time. **(D)** Comparison of the proportion of RBCs with normal morphology in control and PHZ treated mice (N = 6 mice, 1000 randomly selected RBCs counted for each mouse). **(E)** Comparison of the proportion of acanthocytes in control and PHZ treated mice (N = 6 mice, 1000 randomly selected RBCs counted for each). Values are presented as means ± S.E.M; ns, not significant; *, $P < 0.05$.

the proteins potentially associated with α-syn on the RBC membrane were examined by LC-MS/MS. We identified a total of 477 α-syn-associated proteins across 3 independent biological samples, with each sample analyzed in duplicate. Among these, 119 proteins (24.95%) were consistently identified in all 3 biological samples (Supplementary Table 3). To gain insights into the functional roles of these α-syn-associated proteins, we categorized them using the UniProt protein knowledge database based on their molecular function, biological process, molecular pathway, and protein class (**Fig. S5**). The pathway analysis revealed the involvement of 22 pathways, including those related to Parkinson's disease, Huntington's disease, the Apoptosis signaling pathway, the Gonadotropin-releasing hormone receptor pathway, and Glycolysis (Fig. S5D). Categorization based on the protein class of the α-syn-associated proteins revealed 16 distinct classes, including metabolite interconversion enzyme, cytoskeletal protein, chaperone, calcium-binding protein, and defense/immunity protein (Fig. S5C). Importantly, we observed 7 calcium-binding proteins, namely 45 kDa calcium-binding protein, Calmodulin-like protein 5, Annexin A1, Annexin A2, Protein S100-A7, Protein S100-A8, and Protein S100-A9, were associated with α-syn on the RBC membrane.

Aggregated α-syn induced calcium influx

It has been suggested that an increase in intracellular calcium could be the trigger of eryptosis in human erythrocytes [32], leading to cell shrinkage, membrane scrambling, and membrane blebbing [33,34]. Furthermore, alteration in intracellular calcium levels has been associated with neuronal cell death in PD [35,36]. A high level of α-syn can induce calcium entry pathways and contribute to neuronal damage [37–42]. Therefore, we questioned whether aggregated α-syn in RBCs regulated calcium hemostasis, thus leading to morphological changes in RBCs. To test this hypothesis, we

Fig. 5. Aggregated α-syn induced intracellular calcium increase via influx of extracellular calcium. (A) Representative confocal images showing RBCs of WT mice in response to different concentrations of monomeric α-syn at the times indicated during the trace. Scale: 1 μm. **(B)** Traces show calcium dependent fluorescence of RBCs of WT mice in response to different concentrations of monomeric α-syn. N = 20 RBCs from 3 biologically independent experiments. **(C)** Representative confocal images showing RBCs of WT mice in response to different concentrations of aggregated α-syn at the times indicated during the trace. Scale bar: 1 μm. **(D)** Traces show calcium-dependent fluorescence of RBCs of WT mice in response to different concentrations of aggregated α-syn. N = 20 RBCs from 3 biologically independent experiments. **(E)** Representative confocal images showing RBCs of WT mice in response to 0.75 μg/ml aggregated α-syn with PBS as control, with or without Amlodipine, at the time points indicated during the trace. Scale bar: 1 μm. **(F)** Traces show calcium dependent fluorescence of RBCs of WT mice in response to 0.75 μg/ml aggregated α-syn, with or without Amlodipine. N = 20 RBCs from 3 biologically independent experiments. **(G)** Scanning electron micrographs showing RBCs of WT mice treated with 0.75 μg/ml monomeric α-syn (α-syn) and aggregated α-syn (α-syn aggregates), with or without Amlodipine. Scale bar: 2 μm. **(H)** Comparison of the percentage of RBCs of WT mice treated with 0.75 μg/ml monomeric α-syn and aggregated α-syn, with or without Amlodipine (N = 1000). Statistical significance was determined for the percentage of normal RBCs between certain groups via Student's *t*-test. Values are means ± S.E.M; ns, not significant; *, $P < 0.05$.

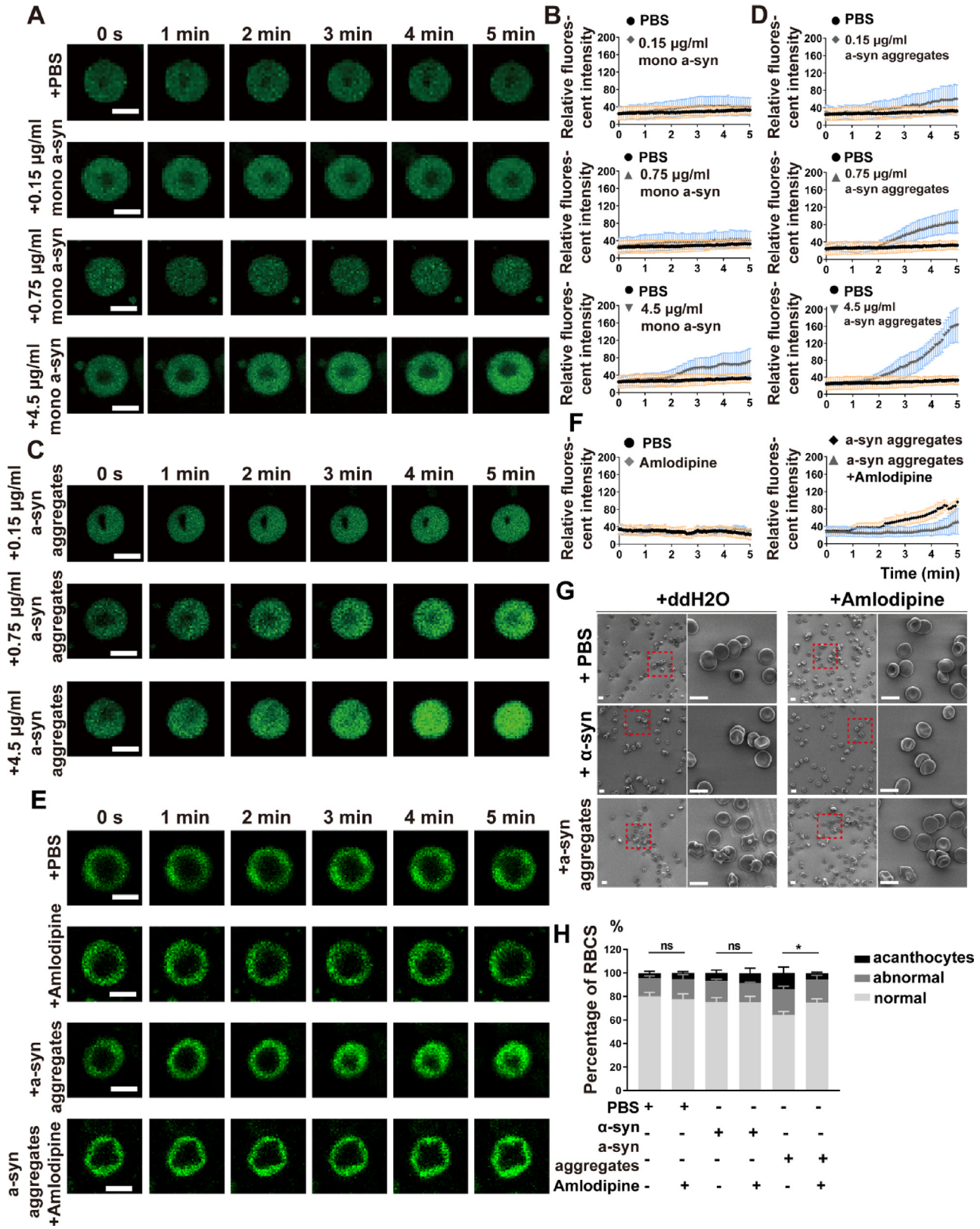
A
0 s
1 min
2 min
3 min
4 min
5 min
+PBS
+0.15 μg/ml mono a-syn
+0.75 μg/ml mono a-syn
+4.5 μg/ml mono a-syn
B
PBS
0.15 μg/ml mono a-syn
0.75 μg/ml mono a-syn
4.5 μg/ml mono a-syn
Relative fluorescent intensity
D
PBS
0.15 μg/ml a-syn aggregates
0.75 μg/ml a-syn aggregates
4.5 μg/ml a-syn aggregates
C
+0.15 μg/ml a-syn aggregates
+0.75 μg/ml a-syn aggregates
+4.5 μg/ml a-syn aggregates
F
PBS
Amlodipine
a-syn aggregates
a-syn aggregates +Amlodipine
Time (min)
E
+PBS
+Amlodipine
+a-syn aggregates
a-syn aggregates +Amlodipine
G
+ddH2O
+Amlodipine
+ PBS
+ α-syn
+a-syn aggregates
H
Percentage of RBCS
%
ns
ns
*
acanthocytes
abnormal
normal
PBS
α-syn
a-syn aggregates
Amlodipine

monitored calcium signal in RBCs loaded with calcium-dependent fluorescence fluo-4 upon exposure to monomeric or aggregated α-syn. No difference in calcium signal was observed when RBCs from 3-month-old WT mice were treated with monomeric α-syn vs. PBS, except at the highest concentration of α-syn (4.5 μg/ml) (Fig. 5**A and 5B**). In contrast to monomeric α-syn, aggregated α-syn evoked a rapid, dose-dependent increase of calcium signal within minutes (Fig. 5**C and 5D**). In the absence of extracellular calcium, using calcium-free buffer, the intracellular calcium increase induced by aggregated α-syn was completely abrogated (**Fig. S6**). These findings suggest that aggregated α-syn and high levels of monomeric α-syn were able to trigger an increase in intracellular calcium in RBCs from an extracellular calcium source.

Aggregated α-syn affected RBC morphology through calcium influx

To further investigate how aggregated α-syn impacts RBC morphology through calcium influx, we added Amlodipine (an L-type calcium channel inhibitor), ω-Conotoxin GVIA TFA (an N-type calcium channel inhibitor), or Fendiline hydrochloride (a nonselective calcium channel blocker) to RBCs before incubation with 0.75 μg/ml aggregated α-syn. While the magnitude of the signal response in the presence of ω-Conotoxin GVIA TFA and Fendiline hydrochloride was comparable to that obtained in their absence (**Fig. S7**), Amlodipine significantly abrogated the intracellular calcium increase induced by aggregated α-syn (Fig. 5**E and 5F**), suggesting that calcium influx through L-type calcium channel contributes to the aggregated α-syn-induced intracellular calcium increase. Remarkably, following the treatment with Amlodipine, the morphological alternations in aggregated-α-syn-treated WT RBCs were significantly rescued (Fig. 5**G and 5H**). These results suggest that aggregated α-syn induces extracellular calcium influx, thus leading to changes in the morphology of RBCs.

Discussion

This investigation has yielded several novel observations. First, compared to healthy controls and other neurodegenerative disorders (e.g., AD), PD patients exhibited significant alterations in the morphology of their RBCs, including the presence of surface protrusions or the formation of acanthocytes. This observation not only validates previous reports [16] but also suggests that the observed morphological alterations in PD are likely specific to the disease. It's worth noting that changes in RBC morphology have also been reported in AD patients [43]; however, at least in terms of the major change observed in our study (formation of acanthocytes), PD appears to differ significantly from AD. Furthermore, our study suggests that an excess of aggregated α-syn on the RBC membrane may be primarily responsible for the changes unique to PD. However, due to the limited number of patients included in the study, it is necessary to validate the key observations in a larger group of patients in further investigations. Additionally, it is worth noting that a significant portion of the recruited patients lacked comprehensive records of the total dopamine or related medications received at the time of blood collection. In future studies, it is critical to investigate the potential impact of varying levels of dopamine or related medications on the morphology of RBCs in PD patients.

The second significant advancement lies in demonstrating the correlation between the level of membrane-bound aggregated α-syn and RBC morphology. We conducted a comparison of the levels of aggregated α-syn on the RBC membrane in PD patients and healthy controls, as well as between A53T and WT mice. The results revealed that both PD patients and A53T mice exhibited significantly higher levels of aggregated α-syn on their RBC membranes compared to the control groups. Previous studies have demonstrated elevated levels of total α-syn in RBCs of PD patients compared to controls [44], and the ratio of aggregated α-syn to total RBC protein was higher in PD patients [12]. More recent research has identified significantly increased levels of α-syn dimers on the RBC membrane in PD patients [45]. Furthermore, a cohort study involving 225 PD patients and 133 healthy controls demonstrated markedly elevated levels of total α-syn, pS129 α-syn, and aggregated α-syn on the RBC membrane in PD patients [8]. The findings presented in this study align with these previous results, demonstrating that the levels of aggregated α-syn on the RBC membrane in both PD patients and A53T mice were significantly higher than those in the control groups. Given the significant differences in RBC morphology observed in PD patients and A53T mice compared to controls, we hypothesized that the aggregated α-syn on the RBC membrane in PD may contribute to the abnormal RBC morphology.

To further confirm a critical role of α-syn in RBC morphology, the effects of α-syn on the morphology of RBCs were investigated using SNCA-KO mice, which showed a lower proportion of acanthocytes compared to WT mice. The *in vitro* culture of RBCs from WT, SNCA-KO, and A53T mice treated with monomeric and aggregated α-syn, along with *in vivo* acute hemolysis induced by PHZ in mice, further demonstrated the correlation between the level of aggregated α-syn on the RBC membrane and the proportion of RBC morphological abnormalities. Of note, previous study reported abnormal RBC morphology in PD patients and hypothesized that peripheral inflammation, increased iron levels, and elevated serum ferritin levels could be contributing factors [16]. To this end, the effects of α-syn and peripheral inflammation may not be mutually exclusive, particularly considering the known effects of aggregated α-syn on inflammation [24].

In the present study, the difference in RBC morphology could be detected in 3-month-old A53T mice, while the subtle motor behavior abnormalities could only be detected in this PD model between 6 and 12 months of age, suggesting the biological importance of RBCs in the early development and progression of PD. This is supported by a recent population-based cohort study that demonstrated that, within a mean follow-up period of 6.6 years, newly diagnosed anemic patients were at a higher risk of PD compared to non-anemic controls [17]. Also, notably, the A53T mice utilized in this study predominantly exhibited peripheral pathology, with α-syn protein levels in the brain showing only a 1–1.5-fold increase compared to WT mice. This observation may provide an explanation for why we detected RBC morphological abnormalities occurring earlier than motor behavior abnormalities. Nonetheless, to gain deeper insights into the role of RBC-derived α-syn in the progression of PD, prospective PD cohorts are essential for monitoring morphological changes and α-syn levels in RBCs at various disease stages.

The final major result relates to the identification of a mechanism that is likely responsible for the α-syn-mediated alterations on the RBC morphology. This process commenced with LC-MS/MS analysis, identifying 119 proteins associated with α-syn in 3 independent biological samples. Among these, 7 proteins, including 45 kDa calcium-binding protein, Calmodulin-like protein 5, Annexin A1, Annexin A2, Protein S100-A7, Protein S100-A8, and Protein S100-A9, belonged to the category of calcium-binding proteins. They can bind to Ca^{2+} and act as Ca^{2+} delivery proteins and chaperones, thus regulating calcium homeostasis [46]. Previous studies reported that the increase of intracellular Ca^{2+} may trigger eryptosis in human erythrocytes [32], leading to cell shrinkage, membrane scrambling and membrane blebbing [33,34]. In this study, we observed aggregated α-syn could evoke a rapid dose-dependent increase of Ca^{2+} signals in RBCs within minutes, which could be eliminated by Amlodipine, a L-type Ca^{2+}channel inhibitor.

Furthermore, the addition of Amlodipine significantly rescued the morphological changes in WT RBCs treated with aggregated α-syn. Notably, prior research by Adamczyk *et al.* reported that monomeric α-syn could induce Ca^{2+} influx in rat synaptoneurosomes, which could be eliminated by ω-conotoxin GVIA, an N-type Ca^{2+}-channel inhibitor [47]. Meanwhile, Danzer *et al.* suggested that homemade α-syn aggregates could induce calcium influx in SH-SY5Y, independent of cobalt-sensitive calcium channels [48]. These two studies are different from our studies in two species. First, they used different α-syn species (monomeric α-syn or α-syn aggregates generated under different conditions, and second, they investigated the calcium influx in different cell types (rat synaptoneurosomes, human neuron cell SH-SY5Y, and RBC). Therefore, these two studies are not in direct contradiction to our findings and provide complementary insights into the calcium-related effects of α-syn in different contexts and cell types.

Regarding the mechanism underlining the increased calcium influx induced by aggregated α-syn in RBC, previous studies reported that α-syn can interact with lipid membrane and aggregation of α-syn on the membrane can disrupt membrane integrity [20,21]. Additionally, Fusco *et al.* reported that α-syn aggregates can form a structured region to insert into lipid bilayers, perturb membrane integrity and increase calcium influx in SH-SY5Y cells [23]. Furthermore, it is also possible that aggregated α-syn directly interacts with calcium-binding proteins to regulate calcium homeostasis. Nonetheless, the precise mechanisms involved in the increased calcium influx in RBC induced by aggregated α-syn, including membrane integrity disruption and direct interaction with calcium-binding proteins, need to be investigated further.

Conclusion

Taken together, we found the RBC morphology of PD patients commonly exhibited changes, characterized by an increased presence of acanthocytes. The lower percentage of normally shaped RBCs in patients with PD compared to those with other neurological disorders suggests specific morphological changes in RBCs in PD patients, rather than a general effect of neurodegeneration. Further study revealed that elevated aggregated α-syn on the RBC membrane may induce extracellular calcium influx, leading to changes in RBC morphology in PD. This study proposes a mechanism by which α-syn, a key protein in PD, regulates RBC morphology, providing a potential new avenue for exploring the pathogenesis of α-syn and establishing a theoretical basis for the discovering blood-based biomarkers for early diagnosis of PD.

Ethics approval and consent to participate

The study was approved by the Clinical Research Ethics Committee of the First Affiliated Hospital, Zhejiang University School of Medicine (No. IIT20200473A). All participants gave written informed consent before blood sampling.

Availability of data and materials

The authors confirm that the data supporting the findings of this study are available within the article and its supplementary material.

Funding

National Natural Science Foundation of China 82020108012 (JZ).

National Natural Science Foundation of China 82001200 (YY).

Leading Innovation and entrepreneurship Team of Zhejiang Province 2020R01001 (JZ).

Natural Science Foundation of Zhejiang Province LZ23H090002 (YY).

National Natural Science Foundation of China 81571226 (JZ).

National Natural Science Foundation of China 81671187 (JZ).

Innovative Institute of Basic Medical Science of Zhejiang University (JZ).

Consent for publication

Not applicable

CRediT authorship contribution statement

Ying Yang: Investigation, Formal analysis, Methodology, Validation, Visualization, Writing – original draft. **Min Shi:** Writing - review & editing. **Xiaodan Liu:** Investigation. **Qiaoyun Zhu:** Investigation. **Zhi Xu:** Investigation. **Genliang Liu:** Investigation. **Tao Feng:** Writing – review & editing. **Tessandra Stewart:** Writing – review & editing. **Jing Zhang:** Project administration, Conceptualization, Supervision, Funding acquisition, Writing – review & editing.

Declaration of Competing Interest

The authors declare that they have no known competing financial interests or personal relationships that could have appeared to influence the work reported in this paper.

Acknowledgments

We deeply appreciate the participants for their generous donation of samples.

Appendix A. Supplementary material

Supplementary data to this article can be found online at https://doi.org/10.1016/j.jare.2023.09.009.

References

[1] Grayson M. Parkinson's disease. Nature 2016;538(7626):S1.
[2] Bloem BR, Okun MS, Klein C. Parkinson's disease. Lancet 2021;397 (10291):2284–303.
[3] Costa HN, Esteves AR, Empadinhas N, Cardoso SM. Parkinson's Disease: A Multisystem Disorder. Neurosci Bull 2023;39(1):113–24.
[4] Spillantini MG, Schmidt ML, Lee VM, Trojanowski JQ, Jakes R, Goedert M. Alpha-synuclein in Lewy bodies. Nature 1997;388(6645):839–40.
[5] Tofaris GK. Initiation and progression of α-synuclein pathology in Parkinson's disease. Cell Mol Life Sci 2022;79(4):210.
[6] Barbour R, Kling K, Anderson JP, Banducci K, Cole T, Diep L, et al. Red blood cells are the major source of alpha-synuclein in blood. Neurodegener Dis 2008;5 (2):55–9.
[7] Shi M, Zabetian CP, Hancock AM, Ginghina C, Hong Z, Yearout D, et al. Significance and confounders of peripheral DJ-1 and alpha-synuclein in Parkinson's disease. Neurosci Lett 2010;480(1):78–82.
[8] Tian C, Liu G, Gao L, Soltys D, Pan C, Stewart T, et al. Erythrocytic α-Synuclein as a potential biomarker for Parkinson's disease. Transl Neurodegener 2019;8:15.
[9] Winner B, Jappelli R, Maji SK, Desplats PA, Boyer L, Aigner S, et al. In vivo demonstration that alpha-synuclein oligomers are toxic. Proc Natl Acad Sci U S A 2011;108(10):4194–9.
[10] Deas E, Cremades N, Angelova PR, Ludtmann MH, Yao Z, Chen S, et al. Alpha-Synuclein Oligomers Interact with Metal Ions to Induce Oxidative Stress and Neuronal Death in Parkinson's Disease. Antioxid Redox Signal 2016;24 (7):376–91.
[11] Roberts HL, Brown DR. Seeking a mechanism for the toxicity of oligomeric α-synuclein. Biomolecules 2015;5(2):282–305.
[12] Wang X, Yu S, Li F, Feng T. Detection of α-synuclein oligomers in red blood cells as a potential biomarker of Parkinson's disease. Neurosci Lett 2015;599:115–9.

[13] Zhao HQ, Li FF, Wang Z, Wang XM, Feng T. A comparative study of the amount of α-synuclein in ischemic stroke and Parkinson's disease. Neurol Sci 2016;37(5):749–54.
[14] Sulzer D, Edwards RH. The physiological role of α-synuclein and its relationship to Parkinson's Disease. J Neurochem 2019;150(5):475–86.
[15] Bernal-Conde LD, Ramos-Acevedo R, Reyes-Hernández MA, Balbuena-Olvera AJ, Morales-Moreno ID, Argüero-Sánchez R, et al. Alpha-Synuclein Physiology and Pathology: A Perspective on Cellular Structures and Organelles. Front Neurosci 2019;13:1399.
[16] Pretorius E, Swanepoel AC, Buys AV, Vermeulen N, Duim W, Kell DB. Eryptosis as a marker of Parkinson's disease. Aging (Albany NY) 2014;6(10):788–819.
[17] Hong CT, Huang YH, Liu HY, Chiou HY, Chan L, Chien LN. Newly Diagnosed Anemia Increases Risk of Parkinson's disease: A Population-Based Cohort Study. Sci Rep 2016;6:29651.
[18] Savica R, Grossardt BR, Carlin JM, Icen M, Bower JH, Ahlskog JE, et al. Anemia or low hemoglobin levels preceding Parkinson disease: a case-control study. Neurology 2009;73(17):1381–7.
[19] Wang YC, Huang AP, Yuan SP, Huang CY, Wu CC, Poly TN, et al. Association between Anemia and Risk of Parkinson Disease. Behav Neurol 2021;2021:8360627.
[20] Reynolds NP, Soragni A, Rabe M, Verdes D, Liverani E, Handschin S, et al. Mechanism of membrane interaction and disruption by α-synuclein. J Am Chem Soc 2011;133(48):19366–75.
[21] Auluck PK, Caraveo G, Lindquist S. α-Synuclein: membrane interactions and toxicity in Parkinson's disease. Annu Rev Cell Dev Biol 2010;26:211–33.
[22] Froula JM, Castellana-Cruz M, Anabtawi NM, Camino JD, Chen SW, Thrasher DR, et al. Defining α-synuclein species responsible for Parkinson's disease phenotypes in mice. J Biol Chem 2019;294(27):10392–406.
[23] Fusco G, Chen SW, Williamson PTF, Cascella R, Perni M, Jarvis JA, et al. Structural basis of membrane disruption and cellular toxicity by α-synuclein oligomers. Science 2017;358(6369):1440–3.
[24] Liu Z, Chan RB, Cai Z, Liu X, Wu Y, Yu Z, et al. α-Synuclein-containing erythrocytic extracellular vesicles: essential contributors to hyperactivation of monocytes in Parkinson's disease. J Neuroinflamm 2022;19(1):53.
[25] Zhang W, Wang T, Pei Z, Miller DS, Wu X, Block ML, et al. Aggregated alpha-synuclein activates microglia: a process leading to disease progression in Parkinson's disease. Faseb J 2005;19(6):533–42.
[26] Sano K, Atarashi R, Satoh K, Ishibashi D, Nakagaki T, Iwasaki Y, et al. Prion-Like Seeding of Misfolded α-Synuclein in the Brains of Dementia with Lewy Body Patients in RT-QUIC. Mol Neurobiol 2018;55(5):3916–30.
[27] Fairfoul G, McGuire LI, Pal S, Ironside JW, Neumann J, Christie S, et al. Alpha-synuclein RT-QuIC in the CSF of patients with alpha-synucleinopathies. Ann Clin Transl Neurol 2016;3(10):812–8.
[28] Garrido A, Fairfoul G, Tolosa E, Marti MJ, Ezquerra M, Green AJE. Brain and Cerebrospinal Fluid α-Synuclein Real-Time Quaking-Induced Conversion Identifies Lewy Body Pathology in LRRK2-PD. Mov Disord 2023;38(2):333–8.
[29] Kuo YM, Li Z, Jiao Y, Gaborit N, Pani AK, Orrison BM, et al. Extensive enteric nervous system abnormalities in mice transgenic for artificial chromosomes containing Parkinson disease-associated alpha-synuclein gene mutations precede central nervous system changes. Hum Mol Genet 2010;19(9):1633–50.
[30] Hu P, Nebreda AR, Hanenberg H, Kinnebrew GH, Ivan M, Yoder MC, et al. P38α/JNK signaling restrains erythropoiesis by suppressing Ezh2-mediated epigenetic silencing of Bim. Nat Commun 2018;9(1):3518.
[31] Unami A, Nishina N, Terai T, Sato S, Tamura T, Noda K, et al. Effects of cisplatin on erythropoietin production in rats. J Toxicol Sci 1996;21(3):157–65.
[32] Gao M, Lau PM, Kong SK. Mitochondrial toxin betulinic acid induces in vitro eryptosis in human red blood cells through membrane permeabilization. Arch Toxicol 2014;88(3):755–68.
[33] Lang F, Lang E, Föller M. Physiology and pathophysiology of eryptosis. Transfus Med Hemother 2012;39(5):308–14.
[34] Lang F, Abed M, Lang E, Föller M. Oxidative stress and suicidal erythrocyte death. Antioxid Redox Signal 2014;21(1):138–53.
[35] Arshad A, Chen X, Cong Z, Qing H, Deng Y. TRPC1 protects dopaminergic SH-SY5Y cells from MPP+, salsolinol, and N-methyl-(R)-salsolinol-induced cytotoxicity. Acta Biochim Biophys Sin (Shanghai) 2014;46(1):22–30.
[36] Yoshida I, Monji A, Tashiro K, Nakamura K, Inoue R, Kanba S. Depletion of intracellular Ca2+ store itself may be a major factor in thapsigargin-induced ER stress and apoptosis in PC12 cells. Neurochem Int 2006;48(8):696–702.
[37] Betzer C, Lassen LB, Olsen A, Kofoed RH, Reimer L, Gregersen E, et al. Alpha-synuclein aggregates activate calcium pump SERCA leading to calcium dysregulation. EMBO Rep 2018;19(5).
[38] Caraveo G, Auluck PK, Whitesell L, Chung CY, Baru V, Mosharov EV, et al. Calcineurin determines toxic versus beneficial responses to α-synuclein. Proc Natl Acad Sci U S A 2014;111(34):E3544–52.
[39] Mironov SL. α-Synuclein forms non-selective cation channels and stimulates ATP-sensitive potassium channels in hippocampal neurons. J Physiol 2015;593(1):145–59.
[40] Lieberman OJ, Choi SJ, Kanter E, Saverchenko A, Frier MD, Fiore GM, et al. α-Synuclein-Dependent Calcium Entry Underlies Differential Sensitivity of Cultured SN and VTA Dopaminergic Neurons to a Parkinsonian Neurotoxin. eNeuro 2017;4(6).
[41] Hettiarachchi NT, Parker A, Dallas ML, Pennington K, Hung CC, Pearson HA, et al. alpha-Synuclein modulation of Ca2+ signaling in human neuroblastoma (SH-SY5Y) cells. J Neurochem 2009;111(5):1192–201.
[42] Angelova PR, Ludtmann MH, Horrocks MH, Negoda A, Cremades N, Klenerman D, et al. Ca2+ is a key factor in α-synuclein-induced neurotoxicity. J Cell Sci 2016;129(9):1792–801.
[43] Bester J, Buys AV, Lipinski B, Kell DB, Pretorius E. High ferritin levels have major effects on the morphology of erythrocytes in Alzheimer's disease. Front Aging Neurosci 2013;5:88.
[44] Wang L, Wang G, Duan Y, Wang F, Lin S, Zhang F, et al. A Comparative Study of the Diagnostic Potential of Plasma and Erythrocytic α-Synuclein in Parkinson's Disease. Neurodegener Dis 2019;19(5–6):204–10.
[45] Papagiannakis N, Koros C, Stamelou M, Simitsi AM, Maniati M, Antonelou R, et al. Alpha-synuclein dimerization in erythrocytes of patients with genetic and non-genetic forms of Parkinson's Disease. Neurosci Lett 2018;672:145–9.
[46] Yáñez M, Gil-Longo J, Campos-Toimil M. Calcium binding proteins. Adv Exp Med Biol 2012;740:461–82.
[47] Adamczyk A, Strosznajder JB. Alpha-synuclein potentiates Ca2+ influx through voltage-dependent Ca2+ channels. Neuroreport 2006;17(18):1883–6.
[48] Danzer KM, Haasen D, Karow AR, Moussaud S, Habeck M, Giese A, et al. Different species of alpha-synuclein oligomers induce calcium influx and seeding. J Neurosci 2007;27(34):9220–32.